Voltage and Frequency Control of Wind-Powered Islanded Microgrids based on Induction Generator and STATCOM

Allal.M Bouzid[1,3], Pierre Sicard[1,] Ahmed Cheriti[1], Josep M. Guerrero[2], Mohamed Bouhamida[3], Mohammad S. Golsorkhi[4]

[1] Department of Electrical & Computer Engineering Université du Québec à Trois-Rivières (Québec), Canada

[2] Department of Energy Technology, Aalborg University, Aalborg East 9220, Denmark

[3] Department of Electrical Engineering, Université des Sciences et de la Technologie d'Oran, Algeria

[4] The School of Electrical and Information Engineering, The University of Sydney, Australia

Allal.El.Moubarek.Bouzid@uqtr.ca, Pierre.Sicard@uqtr.ca, joz@et.aau.dk, mohammad.golsorkhiesfahani@sydney.edu.au

Abstract—**This paper presents a comprehensive modeling of a three-phase cage induction machine used as a self-excited squirrel-cage induction generator (SEIG), and discusses the regulation of the voltage and frequency of a self-excited SEIG based on the action of the static synchronous Compensator (STATCOM). The STATCOM with the proposed controller consists of a three-phase voltage-sourced inverter and a DC voltage. The compensator can provide the active and reactive powers and regulate AC system bus voltage and the frequency, but also may enhance the load stability. Moreover, a feed forward control method for the STATCOM is introduced and applied for controlling the SEIG's terminal voltage using a two-degree of freedom RST controller. Simulation results for the steady-state operating condition and transient operating conditions for the system subjected to a wind reference step change, and a step load change are presented to demonstrate the effectiveness of the proposed controller.**

Keywords— STATCOM, voltage control, frequency control, islanded generation, induction generator

I. INTRODUCTION

Due to the rapid depletion of conventional fuels and the quick growth of environmental protection concepts, renewable energy sources have been extensively developed and studied in the whole world. Wind, bio, hydro and solar energy are in the forefront with fairly mature technologies adaptable to the field [1]. Wind energy is, for many reasons, one of the most promising renewable energy sources; it comprises a wind turbine, an electric generator, a power electronic converter and the corresponding control system [2]. In this sense, self-excited induction generators (SEIG) are good candidates for wind powered electricity generation especially in remote areas, because they do not need an external power supply to produce the excitation magnetic field [3]. The performance of voltage and frequency in isolated induction generator may vary according to the speed of the rotor and the load connected to the generator, due to a decrease in the speed of the rotating magnetic field [4]. The wind turbine can be designed to operate at a constant speed or variable speed. The frequency of the isolated induction generator varies with the load demand, and therefore its application should be to supply equipment

insensitive to frequency variations, such as heaters, water pumps, lighting, charging battery, etc. But the major disadvantage of SEIG, is its poor voltage and frequency regulation under source and load perturbations, which may limit its use in isolated and scattered generation areas, such as wind and micro hydro renewable energy sources [5]. For applications that require constant voltage and frequency, the stator voltage isolated induction generator should be controlled to stay at a given reference value. A SEIG can be controlled by varying the rotor resistance of a SEIG sliding ring, but it requires more maintenance than a squirrel cage rotor due to sliding rings [6]. In a SEIG, a rotor squirrel cage is preferable to a wound rotor because the rotor squirrel cage has higher thermal-order potential and require less maintenance [7]. In addition, SEIGs are more robust and cheaper than other electrical machines for the same power rating. They require less maintenance once built with a squirrel-cage. However, at start-up, the induction generator requires a reasonable amount of reactive power which must be fed externally to establish the magnetic field necessary to convert the mechanical power from its shaft into electrical power [3]. This reactive power can be supplied by a bank of capacitors connected across its terminals that must remain permanently connected to the stator windings responsible for the output voltage control [8]. Fig.1 shows the stator side of the generator, a capacitor bank used for the excitation, the STATCOM, and the consumer load.
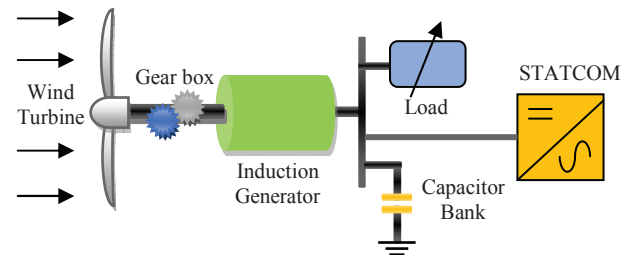

Fig. 1. Diagram of the islanded microgrid based on SEIG with STATCOM

This paper introduces a voltage and frequency control of a wind-power islanded microgrid by using a STATCOM. A mathematical model of the proposed system is developed. The STATCOM is controlled by using a feed-forward and two

feedback control loops. The RST controller is proposed in order to obtain a good performance. Therefore, a control scheme is required to regulate the output voltage to meet the constant voltage demand. The simulation results using MATLAB® environment are carried out and thoroughly discussed and included in this paper

II. MATHEMATICAL MODEL OF A SEIG

The modeling of the three-phase squirrel cage induction generator is performed through the Clarke and Park transformations in the synchronously rotating reference frames and the relevant volt-ampere equations are written as [9] (variable are defined in Appendix):

$$[V] = [R][I] + [L]\frac{d}{dt}[I] + \omega_r[G][I] \qquad (1)$$

from which, the current derivative can be expressed as:

$$\frac{d}{dt}[I] = [L]^{-1}\{[V] - [R][I] - \omega_r[G][I]\} \qquad (2)$$

$$\frac{d}{dt}[I] = -[L]^{-1}\{[R][I] + \omega_r[G][I] - [V]\} \qquad (3)$$

A. Magnetizing inductance

The SEIG operates in the saturation region and its magnetizing characteristics are non-linear in nature. The magnetizing current should be calculated at every step of integration in terms of the stator and rotor d-q currents as:

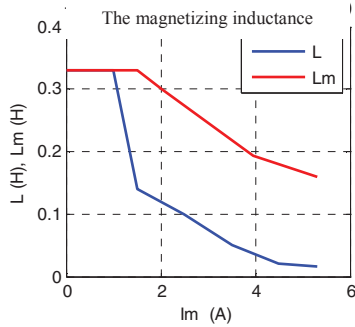$$I_m = \sqrt{(I_{ds} + I_{dr})^2 + \left(I_{qs} + I_{qr}\right)^2} \qquad (4)$$

Fig. 2. Comparative study between linear and saturation state

Fig. 2 shows the evolution of magnetizing inductance L_m and dynamic inductance L as a function of the magnetizing current I_M module of SEIG. When the operating point is reached, the machine delivers a voltage to the stator, which effective value is constant. The simulation of the phenomenon of self-excitation of the asynchronous machine with capacitors cannot be achieved with this model since it is the saturation itself that sets the steady state operating point.

The magnetizing inductance is calculated from the magnetizing characteristics and it is obtained by synchronous speed test for the machine. For the test machine rated at 3.5 kW, it is defined as:

$$L_m = 0.63atan(0.15I_m)/I_m \qquad (5)$$

B. Electromagnetic torque

The developed electromagnetic torque T_e of the SEIG is:

$$T_e = (3P/4)L_m\left(I_{qs}I_{dr} - I_{ds}I_{qr}\right) \qquad (6)$$

The Torque balance T_{shaft} equation is:

$$T_{shaft} = T_e + J(2/P)\frac{d}{dt}\omega_r \qquad (7)$$

With P: number of pole pairs; and J : Inertia of the induction machine.

C. Excitation system model

Equations (7) and (8) represent the self-excitation capacitor currents and voltages in d-q axes representation.

$$\begin{cases} I_{ds} = I_{cd} + I_{ld} \\ I_{qs} = I_{cq} + I_{lq} \end{cases} \qquad (8)$$

$$\begin{cases} \frac{d}{dt}V_{ld} = \frac{1}{c_{ex}}I_{ds} - \frac{1}{c_{ex}}I_{ld} \\ \frac{d}{dt}V_{lq} = \frac{1}{c_{ex}}I_{qs} - \frac{1}{c_{ex}}I_{lq} \end{cases} \qquad (9)$$

With I_{cd}, I_{cq} representing the capacitor currents, I_{ld}, I_{lq} representing the grid inductor currents, and C_{ex} representing the capacitor excitation.

D. R-L load model

Equations (10) and (11) represent the d-q axes load voltages and currents.

$$\begin{cases} V_{ld} = RI_{ld} + L\frac{d}{dt}I_{ld} \\ V_{lq} = RI_{lq} + L\frac{d}{dt}I_{lq} \end{cases} \qquad (10)$$

$$\begin{cases} \frac{d}{dt}I_{ld} = \frac{1}{L}V_{ld} - \frac{R}{L}I_{ld} \\ \frac{d}{dt}I_{lq} = \frac{1}{L}V_{lq} - \frac{R}{L}I_{lq} \end{cases} \qquad (11)$$

III. SYSTEM CONFIGURATION AND CONTROL SCHEME

The STATic COMpensator (STATCOM) is designed to regulate the line voltage at the Point of Common Coupling (PCC), by injecting or absorbing a certain amount of reactive power. It can balance loads or compensate load reactive power by producing the desired amplitude and phase of inverter output voltage [10]; it may also be used for additional tasks such as stabilization of power system. The STATCOM is playing increasingly important roles in reactive power provision, which is why it receives considerable attention due to the urgent requirement for tackling the voltage fluctuation problems. The topology of the SEIG - STATCOM presented in this paper is depicted in Fig.3. The compensator consists of a voltage source converter, a DC voltage, an inductance, L_{sh} (representing the leakage inductance of the transformer and line) and a resistor, R_{sh} (representing the inverter and transformer conduction losses) on the AC side. STATCOM is connected in parallel with a fixed capacitor and load. In order to obtain a rated voltage at no load, the suitable capacitor bank is needed. Synchronous frame (dq) control is used so that the reference currents that control the reactive power and consequently the generated voltage become simple, effective and easy to tune. Feed forward loops of id^*, iq^* and Vq are

used to minimize the coupling effect between *id* and *iq*. The voltage at the DC bus is relatively smooth due to the battery [11, 12].

A. Voltage and frequency control

The voltage control is performed according to the following steps:

- The regulation of the load voltage/frequency is performed by comparing the actual voltage/frequency to a desired reference value.

- The error between the two voltages goes through a PI controller.

- By the action of the PI controller, the reference current $i_d{}^*$ and $i_q{}^*$ are generated and consequently control the active / reactive power.
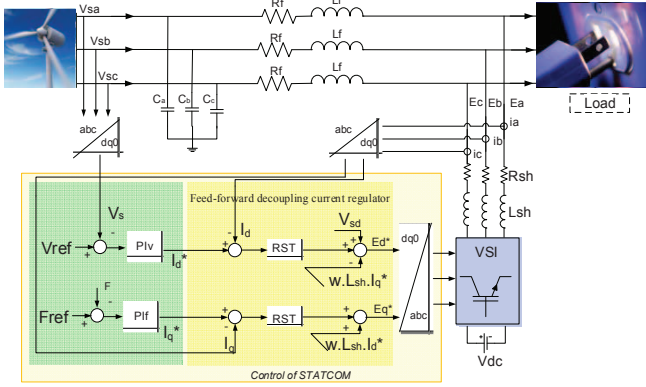
Fig. 3.   Control scheme for STATCOM - SEIG system.

B. Control of the inner loop (current loop)

The equivalent circuit models of the STATCOM on d-q reference frame for both loops of the circuit d-axis and q-axis are shown in Fig. 4 (a) and (b) for synthesis of the proper parameters for the current regulator, the AC voltage controller and the frequency controller. The system is based on the equations (12) (13) as follows:

$$E_d = -\omega L_{sh} I_q + R_{sh} I_d + L_{sh} \frac{dI_d}{dt} + V_d \qquad (12)$$

$$E_q = \omega L_{sh} I_d + R_{sh} I_q + L_{sh} \frac{di_q}{dt} + V_q \qquad (13)$$
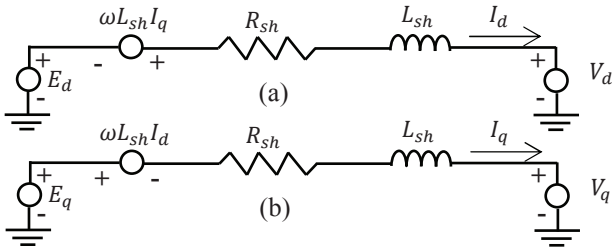
Fig. 4.   Equivalent circuit in dq reference frame of the STATCOM

However, an efficient and easy control system requires the decoupling of the two variables. The current regulator generates the desired STATCOM output voltages E_d^* and E_q^* based on the error current signals $(I_d^* - I_d)$ and $(I_q^* - I_q)$. The

real current reference I_d^* and the reactive current reference I_q^* come from the AC voltage controller and frequency controller, respectively.

The active power P_a and reactive Q power are expressed by

$$Q = \frac{3}{2} Eq\ Id\ ,\ P_a = \frac{3}{2}\ Eq\ Iq \qquad (14)$$

IV.   DESIGN OF THE RST CURRENT CONTROLLER

The objective of this section is to obtain the RST current controller (I_d and I_q). This type of controller is a structure with two degrees of freedom as compared to a one degree of freedom structure. Its main advantage is that it allows the designer to specify performances independently with reference trajectory tracking (reference variation) and with regulation. It is based on the pole placement theory. The RST controller is used with both control loops and it is implemented in continuous form. The block diagram of a system with its RST controller used in the inner loop is shown in Fig 5.
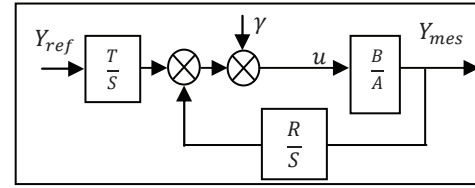
Fig. 5.   RST Structure.

The proposed system is defined by the transfer-function B/A, i has Y_{ref} as a reference and γ as a disturbance. R, S and T are polynomials that constitute the controller. In our case, we have [3, 13]:

$$A = s + R_{sh}/L_{sh} \qquad \text{and} \qquad B = 1/L_{sh} \qquad (15)$$

The closed-loop transfer-function of the controlled system is:

$$Y_{mes} = \frac{B.T}{(A.S+B.R)} Y_{ref} + \frac{B.S}{(A.S+B.R)} \gamma \qquad (16)$$

By applying the Bezout equation, we have

$$D = AS + BR = CF \qquad (17)$$

Where C is the command polynomial and F is the filtering polynomial. In order to have good adjustment accuracy, we choose a strictly proper regulator. So if A is a polynomial of degree n ($deg(A) = n$) we must have:

$$deg(D) = 2n + 1; \quad deg(S) = deg(A) + 1;$$

$$deg(R) = deg(A) \qquad (18)$$

To find the coefficients of polynomials R and S, the robust pole placement method is adopted with T_C as control horizon and T_f as filtering horizon.

$$\begin{cases} A = a_1 s + a_0 \\ B = b_0 \\ D = d_3 s^3 + d_2 s^2 + d_1 s + d_0 \\ R = r_1 s + r_0 \\ S = s_2 s^2 + s_1 s + s_0 \end{cases} \qquad (19)$$

We have $P_C = -1/T_C$ pole of polynomial order C, and $P_f = -1/T_f$ double pole of the polynomial filter F. The pole P_C must improve the speed response of the system and is generally chosen 2–5 times greater than the pole of $P_a = -R_{sh}/L_{sh}$. P_f is generally chosen 3–5 times smaller than P_C. According to the robust pole placement strategy, the polynomial D can be written as:

$$D = \left(s + \frac{1}{T_c}\right)\left(s + \frac{1}{T_f}\right)^2 \qquad (20)$$

$$\begin{cases} P_c = 5P_a = -5\frac{R_{sh}}{L_{sh}} \\ T_c = \frac{1}{3}T_f \end{cases} \qquad (21)$$

To improve the speed response of the system, we adopt the following conditions:

$$D = (s - 5P_a)(s - 15P_a)^2 \qquad (22)$$

By identifying equations (14) and (21), we deduce the coefficients of the polynomial D, which are linked to the coefficients of R and S by the Sylvester matrix . Thus, we can determine the parameters of the RST controller as follows:

$$\begin{cases} d_3 = a_1 s_2 \rightarrow s_2 = \frac{d_3}{a_1} \\ d_2 = a_1 s_1 \rightarrow s_1 = \frac{d_2}{a_1} \\ d_1 = a_0 s_1 + b_0 r_1 \rightarrow r_1 = \frac{d_1 - a_0 s_1}{b_0} \\ d_1 = b_0 r_0 \rightarrow r_0 = \frac{d_0}{b_0} \\ T = r_0 \end{cases} \qquad (23)$$

V. CASE STUDIES

To examine the effectiveness of the proposed STATCOM controller, the system in Fig. 3 was simulated using Matlab®/Simpower and the results are presented. The system parameters used in the simulation are listed in Table I. The residual magnetism in the machine is taken into account in the simulation process without which it is not possible for the generator to self-excite. Initial voltage in the capacitor is also considered. The results obtained for different considerations are as follows.

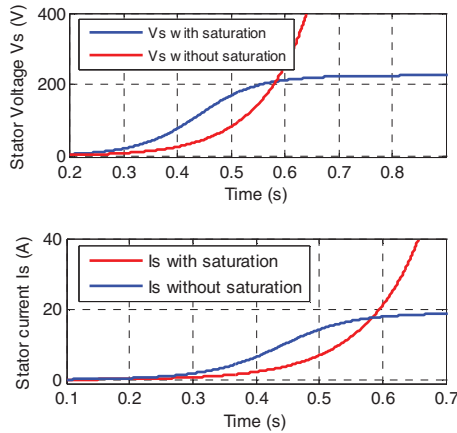### A. Excitation with and without saturation

Fig. 6. Simulation of the SEIG with/without saturation

If the magnetizing inductance is considered as constant and equal to its value in the unsaturated state, the magnetization characteristic then has no saturation bend and there is no intersection with the external characteristic of the capacitor so that the stator variables evolve into the infinite as shown in Fig.6.

To take account of the saturation of the magnetic circuit of the machine, the magnetization curve is necessary; it is generally obtained by experimentation and approximated by a polynomial interpolation. Fig. 7 illustrates the case when the system is started from zero speed. The SEIG is excited with capacitance value C=270µF and value of rotor speed $w_r = 314\ rad/s$ the generated voltage and current attain their steady state values of 220 $Volts$ and 19 A in 0.8 sec, respectively.
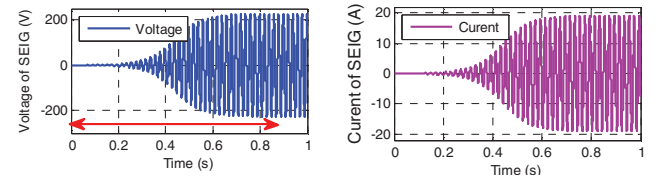

Fig. 7. Simulation of the SEIG with $C_{ex} = 270\mu F$ with saturation

B. Variation of load resistance in steps

In this case, the rotor of the induction machine is driven at 1500 r/min while $C_{ex} = 270\mu F$. The load R is applied to evaluate the performance of the proposed control strategy of the STATCOM. The load resistance is varied in steps.

1) Variations of load without loop control
The load variation range should be small compared with the regulated system to avoid the demagnetization of the SEIG.
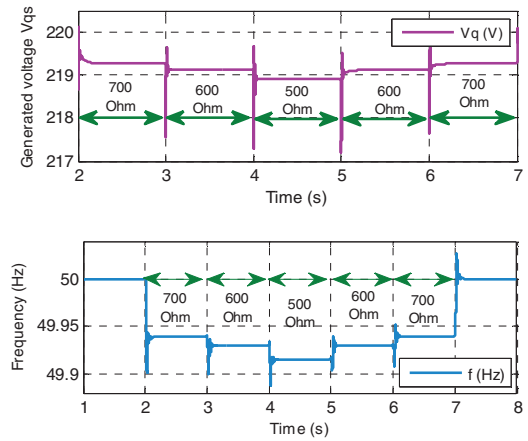

Fig. 8. Effect of load variation on the voltage and frequency

As shown in Fig. 8 the magnitude of the voltage and frequency increases as the load is increased and decreases with the load.

2) Load variation with voltage & frequency control
To test this case, simulation results are shown in Fig. 9. It shows that the STATCOM has very fast dynamic responses. In addition, we observe that the variation of STATCOM current is

also proportional to load changes. For the powers, we note that the variation of P_s is related to the regulation of the frequency and the variation of Q_s is for the voltage regulation. Initially, the system voltage is at its nominal value, P_s and Q_s for (VSI) must be zero, as there is no need for regulation. At time t = 2s we can see that if the frequency decreases the VSI must provide P_s and if it increases then the VSI must absorb P_s. Similarly, if the voltage amplitude decreases the VSI should provide Q_s and vice versa, which keeps the reactive power constant.
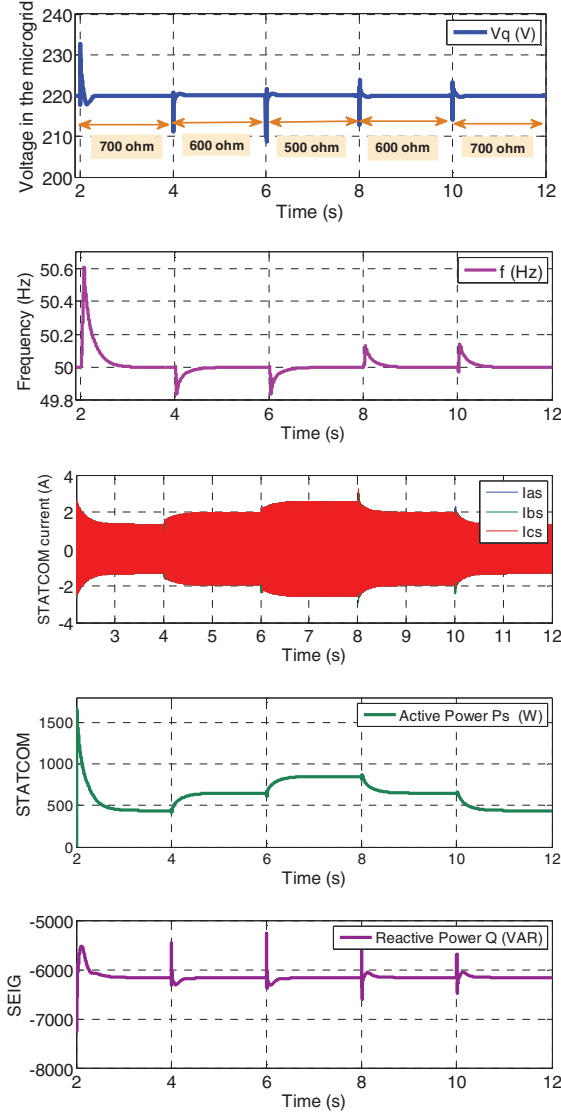

Fig. 9. Performance characteristics of the SEIG-STATCOM with load variation.

C. Voltage control under wind speed variation

In this case, the rotor of the induction machine is driven by speed steps while $C_{ex} = 270\mu F$.

1) Variation of speed without control

At t = 2 s, the rotor speed rises from 315rad/s at to 320 rad/s and down to 310rad/s at t=5s, while the consumer load remains at R = 1KΩ, as shown in Fig. 10. The magnitude of

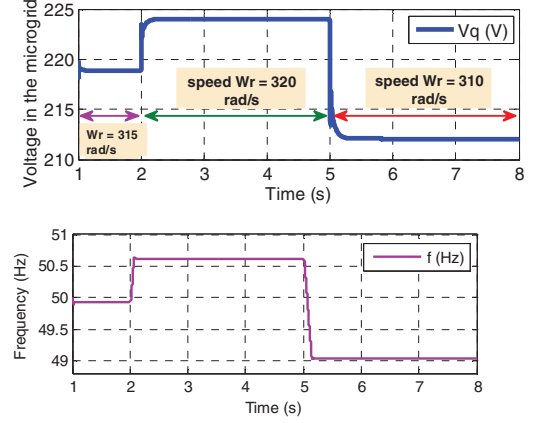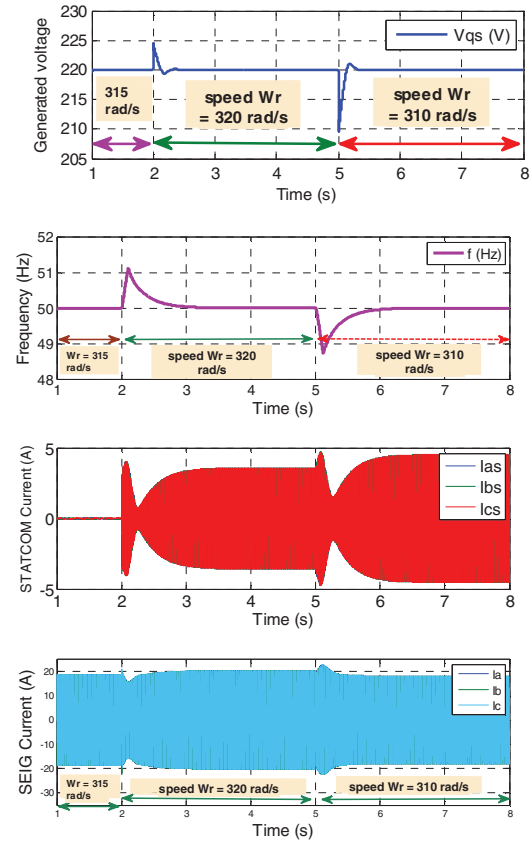the voltage and frequency increases when the speed is increased and decreases when the speed is decreased.

Fig. 10. Effect of wind speed variation on the voltage and frequency

2) Variation of speed with voltage and frequency control

As in the previous case, the voltage and frequency are controlled efficiently (Fig. 11). After transient periods, both the voltage magnitude and frequency return to their rated values as a result of the variation of the reactive power or active power dealt by the compensator. The STATCOM increases the output currents after the wind speed changes but the load voltage and frequency remain constant.

The STATCOM absorbs the necessary amount of power to maintain the voltage constant. As shown in Fig. 11, we conclude that results show that the proposed control system is

effective for the regulation of the voltage and frequency when the wind speed varies.
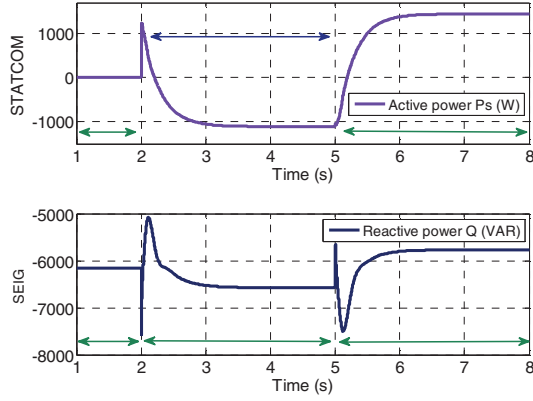

Fig. 11. Performance characteristics of SEIG-STATCOM with wind speed variations.

VI. CONCLUSION

This paper has presented the control of the induction generator using a STATCOM for improving the performance without mechanical turbine control. The control scheme of STATCOM with independent control of its active and reactive powers is proposed. This control can be successfully employed for frequency and voltage magnitude regulation under varying wind speed and load conditions. The results demonstrate that RST controller presents the best performance and the feed forward control enhances the transient response and decoupling of direct and quadratic currents. This work presents some encouraging results that have been determined for the SEIG variable load/ wind speed. The proposed scheme has been verified by simulations results and shows good performance.

APPENDIX

TABLE I. PARAMETERS OF SEIG

Symbol	PARAMETER	Unit
Pm	Rated power of the SEIG	3.5 kW
Vn	Rated voltage of the SEIG	220/380 V
In	Rated current of the SEIG	14/8 A
Rs	Stator resistance	0.76 Ω
Rr	Rotor resistance	0.74 Ω
Lls	Stator Leakage inductance	0.003 H
Llr	Rotor Leakage inductance	0.003 H
Lm	Magnetization inductance	0.074 H
P	Pole pair number	2
f	Frequency	50 Hz
L_m	Magnetizing Inductance	$L_m = 0.63 \tan^{-1}(0.15 I_m)/I_m$

$[V],[I],[R],\ [L]$ and $[G]$ are defined below:

$$L = \begin{bmatrix} L_s & 0 & L_m & 0 \\ 0 & L_s & 0 & L_m \\ L_m & 0 & L_r & 0 \\ 0 & L_m & 0 & L_r \end{bmatrix}; \ G = \begin{bmatrix} 0 & 0 & 0 & 0 \\ 0 & 0 & 0 & 0 \\ 0 & L_m & 0 & L_r \\ -L_m & 0 & -L_r & 0 \end{bmatrix};$$

$$[R] = \begin{bmatrix} R_s & 0 & 0 & 0 \\ 0 & R_s & 0 & 0 \\ 0 & 0 & R_r & 0 \\ 0 & 0 & 0 & R_r \end{bmatrix}; \ [V] = \begin{bmatrix} V_{ds} & V_{qs} & V_{dr} & V_{qr} \end{bmatrix}^T;$$

$$[I] = \begin{bmatrix} I_{ds} & I_{qs} & I_{dr} & I_{qr} \end{bmatrix}^T; \ L_s = L_{ls} + L_m \ ; \ L_r = L_{lr} + L_m$$

REFERENCES

[1] L. Wang and S.-C. Kuo, "Steady state performance of a self-excited induction generator under unbalanced load," in *Power Engineering Society Winter Meeting, 2002. IEEE*, 2002, pp. 408-412.

[2] R. Thakur and V. Agarwal, "Application of interval computation technique to fixed speed wind energy conversion system," in *Sustainable Energy Technologies, 2008. ICSET 2008. IEEE International Conference on*, 2008, pp. 1093-1098.

[3] M. Benghanem, A. Bouzid, M. Bouhamida, and A. Draou, "Voltage control of an isolated self-excited induction generator using static synchronous compensator," *Journal of Renewable and Sustainable Energy*, vol. 5, p. 043118, 2013.

[4] D. Seyoum, C. Grantham, and M. F. Rahman, "The dynamic characteristics of an isolated self-excited induction generator driven by a wind turbine," *IEEE Trans. Ind. Appl.*, vol. 39, pp. 936-944, 2003.

[5] J. Chatterjee, P. Chauhan, P. Murty, and S. Mandal, "Shaft input adaptive source current compensation based novel voltage and frequency control of autonomous induction generator," *International Conference on Power and Energy Systems (ICPS)*, 2011, pp. 1-6.

[6] T. Chan, K. Nigim, and L. Lai, "Voltage and frequency control of self-excited slip-ring induction generators," *Energy Conversion, IEEE Transactions on*, vol. 19, pp. 81-87, 2004.

[7] M. K. Arya, "Steady State Analysis of Self-Excited Induction Generator for Balanced and Unbalanced Conditions," Thapar University Patiala, 2009.

[8] D. Seyoum, C. Grantham, and F. Rahman, "Analysis of an isolated self-excited induction generator driven by a variable speed prime mover," in *Proc. AUPEC*, 2001, pp. 49-54.

[9] Y. K. Chauhan, S. K. Jain, and B. Singh, "Performance of a three-phase self-excited induction generator with static synchronous series compensator," in *Joint International Conference on Power Electronics, Drives and Energy Systems (PEDES) & Power India*, , 2010, pp. 1-6..

[10] N. Farokhnia, R. Khoraminia, and G. Gharehpetian, "Optimization of PI controller gains in nonlinear controller of STATCOM using PSO and GA," in *International conference on Renewable Energies and Power Quality, Granada (Spain), 23rd to 25th March*, 2010.

[11] G. C. Sousa, F. N. Martins, J. P. Rey, and J. A. Bruinsma, "An autonomous induction generator system with voltage regulation," in *Power Electronics and Drive Systems, 2001. Proceedings., 2001 4th IEEE International Conference on*, 2001, pp. 94-98.

[12] G. Dastagir and L. A. Lopes, "Voltage and frequency regulation of a stand-alone self-excited induction generator," in *Electrical Power Conference, 2007. EPC 2007. IEEE Canada*, 2007, pp. 502-506.

[13] B. El Moubarek, "Régulation de la tension d'une génératrice asynchrone auto excitée en utilisant un compensateur statique d'énergie réactive," Ecole Nationale Polytechnique d'Oran, 2012.